

EXPERIMENTAL STUDY AND CFD ANALYSIS OF ENERGY SEPARATION IN A COUNTER FLOW VORTEX TUBE

by

**Lizan Mahmood Khorsheed ZANGANA^{a,b*} and
Ramzi Raphael Ibraheem BARWARI^b**

^a Department of Petroleum Equipment, Erbil Technology Institute,
Erbil Polytechnic University, Kirkuk Road, Erbil, Iraq

^b Mechanics and Mechatronics Department, College of Engineering,
Salahaddin University-Erbil, Erbil, Iraq

Original scientific paper

<https://doi.org/10.2298/TSCI190510418Z>

In this manuscript, both experimental and numerical investigations have been carried out to study the mechanism of separation energy and flow phenomena in the counter flow vortex tube. This manuscript presents a complete comparison between the experimental investigation and CFD analysis. The experimental model was manufactured with (total length of 104 mm and the inner diameter of 8 mm, and made of cast iron) tested under different inlet pressures (4, 5, and 6 bar). The thermal performance has been studied for hot and cold outlet temperature as a function of mass fraction, α , (0.3-0.8). The 3-D numerical modeling using the $k-\epsilon$ model used with code (FLUENT 6.3.26). Two types of velocity components are studied (axial and swirl). The results show any increase in both cold mass fraction and inlet pressure caused to increase ΔT_c , and the maximum ΔT_c value occurs at $P = 6$ bar. The COP of two important factors in the vortex tube which are a heat pump and a refrigerator have been evaluated, which ranged from 0.25 to 0.74. A different axial location ($Z/L = 0.2, 0.5, \text{ and } 0.8$) was modeled to evaluate swirl velocity and radial profiles, where the swirl velocity has the highest value. The maximum axial velocity is 93, where it occurs at the tube axis close to the inlet exit ($Z/L = 0.2$). The results showed a good agreement for experimental and numerical analysis.

Key words: *CFD analysis, experimental study, vortex tube*

Introduction

The essential use of thermodynamics is refrigeration, where the heat is transferred from the low temperature region to the high temperature region with the working fluid named *refrigerant*. Traditional applications in both refrigeration and air-conditioning system are vapour compression and vapour absorption, but the environmental troubles and changes in the atmosphere due to unlike gases such as CFC refrigerants can cause ozone depletion and global warming so that it is necessary to find other non-conventional systems, where natural matter such as air is used as a working medium is the vortex tube [1]. Simply it consists of a straight tube with orifice placed on a diaphragm close to one end, one inlet nozzle with more in some designs, a vortex chamber, a cold-end orifice diameter, a hot-end control valve. The history of the vortex tube back to early in the twentieth century. In 1931, Ranque [2], a French metallurgist, and physicist was granted a French patent for the device in 1932, and a United

* Corresponding author, e-mail: lizan.khorsheed1@gmail.com

States patent in 1934. Ranque [2] was proposing a study about a vortex tube in the subject of dust separation cyclone. He observed an emits of cold air from one side and, hot air from another side. The vortex tube has many applications such as personal air-conditioning, cutting tools shrink fitting, cooling of gas turbine rotor blades, cooling electrical cabinets, cooling of some equipment such as sewing needles, and cooling of hot operations [3]. Vortex tube was desolated for many years until a German engineer Hilsch [4] revived the interesting of this device, who wrote the results of his theoretical studies and comprehensive experimental which led to improving the efficiency of the vortex tube. He studied the influence of the geometrical parameters and the inlet pressure of the vortex tube on its performance also proposed a possible analysis of the process of separation energy. Generally, the vortex tube can be classified as a simple device, which can cause energy separation, *i.e.*, produce two separate flows (hot and cold flows from a single injection of air stream) [5]. In the vortex tube, the air is compressed tangentially, where it separates into two lower pressure streams; the external, and the internal. The rotation of the hot stream will happen near the outer radius of the tube, while the cold stream flows at the core of the tube. The hot, outer part of the compressed gas getaway out of the conical valve at the end of the tube. The residual gas regress in an inner vortex and runs out through the cold exit orifice positioned at another end of the tube close to the inlet. The phenomenon of the vortex tube is shown in fig. 1.

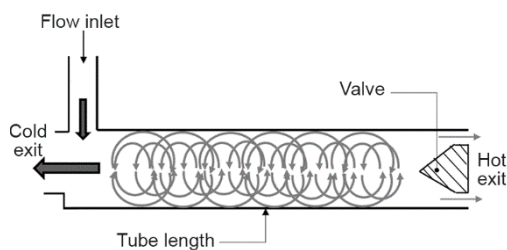


Figure 1. Schematic of vortex tube behavior

The phenomenon theory of the separation temperature in a vortex tube is not wholly recognized until yet because of the complexity. However, various investigators lay many efforts to demonstrate the behavior happening through the separation of energy in the vortex tube. They focused on the geometrical and thermophysical in the experimental study work. Ahlborn and Groves [6] studied secondary flow by using a novel Pitot probe to calculate the axial and azimuthal velocities so

that the study observation showed the turn back stream at the core of the tube is very bigger than the mass of cold which flows grew outside of the cold end. Promvongse and Eiamsa-ard [7] proposed the experimental study of the temperature separation under different geometrical parameters (inlet nozzle, tube insulation, cold orifice diameter, and isentropic efficiency). They showed that the isentropic efficiency is about 30 °C and 33%, respectively, also the maximum temperature separation occurred at four inlet nozzles and 0.5 cold orifice diameter in their work. Aydin and Baki [8] describe design parameters such as the length of the vortex tube, ranged from 250-750 mm, and the inlet nozzle diameter, 5-7 mm, under different inlet pressures with three various working fluids (air, oxygen, and nitrogen). Their results appeared that a rise in the inlet pressure causes a rise in temperature differences. Markal *et al.* [9] considered the influence of the conical angle of the valve (30-75°) on the separation of the energy by designing a modern geometry as a *helical swirl flow generator*. The effect of the valve angle under a different rate of the inlet pressure, 3-5 bar, the helical swirl flow generators lengths are varied from 10 mm to 30 mm, and the length to the diameter L/D ratio ranged from 10 to 40. Their results showed that any decreases in the conical valve angle caused a positive effect on the energy separation. Xue *et al.* [10] performed a new study to determine the dominant cause for the temperature separation with a tube has a huge-scale with a length of 2 m, and 60 mm tube diameter which manufactured to present 3-D velocity distributions using a TFI probe cobra with a precision of

0.3 m/s. Their study showed good agreements between static pressure distributions were measured, and the measured the distribution of pressure stated on the features of vortex forced near the entrance and vortex free at the hot end. The position of the farthest axial velocity showed the variation of the flow structure and supported the assumption of multi-circulation, while the radial velocity distributions appear the external flow from the center nearby the hot end. Aljuwayhel *et al.* [11] used a 2-D axi-symmetric CFD method to examine the vortex tube parametric such as length 10-30 cm, and diameter 1.5 cm and 3 cm where the inlet situations are steady at 300 kPa and 300 K with cold mass fraction 0.3. By using FLUENT software with a mesh consisting of 75000 grids and two turbulence models, *i.e.*, standard $k-\varepsilon$ and RNG $k-\varepsilon$ to study the vortex tube behavior. The CFD models showed three regions of flow as control volumes in the vortex tube: leaving a flow from the hot flow region, leaving a flow from the cold flow region and the re-circulating region flow that circulates nearby the nozzle inlet which is the secondary flow. The CFD model sub-dividing into the control volume related to fluid streams as cold and hot, it can be shown the transfer of work-related with viscous shear happens among the streams and is considerable for the vortex tube's unique phenomenon. The results show the energy separation increases as the length increases, and the angular velocities decrease at the diameter of the vortex tube rises. Eiamsa-ard and Promvonge [12] used 2-D axi-symmetrical solved by finite volume method by using the standard $k-\varepsilon$ turbulence model, and ASM is applied computations model to understand the physical behaviors of the flow, temperature, and pressure in a vortex tube. The results showed that the diffusive transport of mean kinetic energy has a significant effect on the maximum separation of temperature happening nearby the region of the inlet. Farouk and Farouk [13] proposed a CFD model with LES method to suggest the flow fields as effects of a cold mass fraction on the temperature separation. The results showed that the maximum separation of the hot end occurred at a cold mass fraction of 0.78. Pourmahmoud *et al.* [14] used 3-D, $k-\varepsilon$ turbulence model, steady-state, and compressible flow to analyze the effect of inlet gas pressure. The results showed that the acceptable conditions of machine performance could be obtained when the inlet operating pressure is appropriate both to the physical properties of the working fluid and mechanical structure of the machine. Kandil and Abdelghany [15] designed a simulated axisymmetric model using ANSYS FLUENT software to investigate the ratio of the length and the cold orifice to tube diameter influence. The results expressed that the biggest cooling providers at the minimum cold orifice to tube diameter ratio. Niknam *et al.* [16] investigated a 3-D model by using the commercial CFD software ANSYS FLUENT 15 by a hexahedral mesh with refinement near the outlet boundaries to analyze the operating parameters on the Mach number and turbulent viscosity ratio. The results showed the increase in temperature is due to viscous heating, which caused by large swirling flows with a high order of tangential velocity in the circumferential flow. The previous works show the importance of CFD and experimental studies in the development of fundamental phenomena in thermal science [17, 18].

From the invention vortex tube, various explanations were suggested for energy separation. However, because of the nature of the energy separation and complexity of internal flow in the vortex tube, the energy separation phenomenon until now is still unclear. The proposed hypotheses which have been mentioned before can be utilized to discuss the partition of the phenomenon and they do not include all the parts of the temperature separation in the vortex tube because there is not a full study of experimental and numerical analysis to express the behavior. Since most of these studies are based on previous researches to model it or comparison, therefore there has not been a good-reasonable explanation for the separation of thermal still, and the flow behavior inside the vortex tube until now unclear. This paper presents

full fundamental investigations on the Ranque-Hilsch vortex tube, to identify the dominant factors underlying in the energy separation phenomenon based on both the experimental and the numerical studies, which have shown a modern understanding of the flow phenomenon and the process of separation.

Experimental set-up

An experimental investigation has been employed to estimate the influence of operating fluid parameters like pressure on the energy separation inside the vortex tube. In the



Figure 2. Experimental set-up and apparatus parts

present study, the vortex tube (counter flow) has been prepared, fabricated, and examined to evaluate various parameters such as cold and hot exit temperatures, refrigerating effect, and isentropic efficiency. Figure 2 shows the experimental apparatus set-up of the present counter flow vortex tube and the schematic of the current vortex tube set-up has been depicted in fig. 3.

The compressing air is supplied across the compressor storage tank to ensure to get steady pressure with a lower variation. The tank storage has a capacity of 700 L, and the system is working approximately thirty minutes before running the experiments to allow system temperature to stabilize. The highest-rated of the compressor pressure is 6 bars, in the experiments where for inlet pressure varied from 4 to 6 bars, and regulated by a pressure regulator the pressure gauge. The compressed air passed through a filter in order to clean air from particles and residuals to ensure to use of cleanly dry air. Six inlet nozzles, vortex chamber, cold orifice, hot side cone valve, cold and hot ends are used. In the present study, the material used in the vortex tube is manufactured of cast iron with an inner diameter and the length of the tube is 8 mm, 104 mm, respectively. The outlet diameter of the cold side is 5.5 mm as shown in the geometrical design in fig. 4 and tab. 1.

The compressing air is supplied across the compressor storage tank to ensure to get steady pressure with a lower variation. The tank storage has a capacity of 700 L, and the system is working

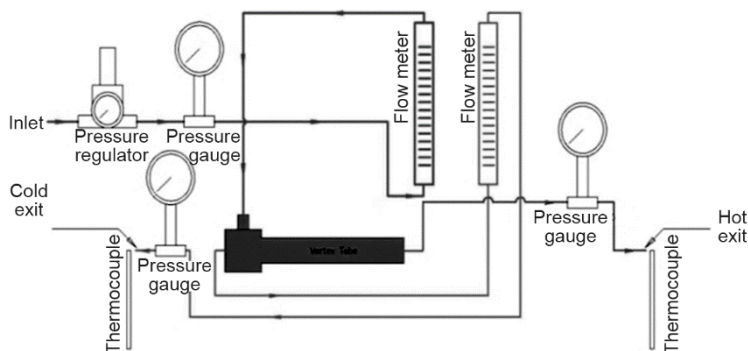


Figure 3. Schematic diagram of experimental set-up

The air is extended in the chamber of the vortex and split into the cold and hot air flows. The cold flow in the center part goes out of the tube across the center orifice nearby to

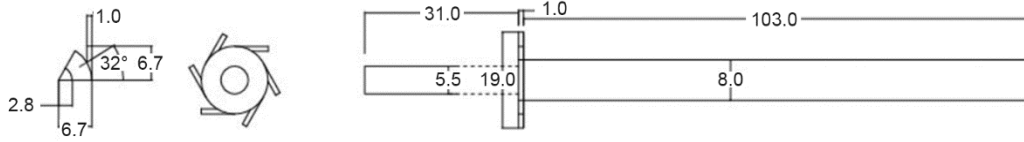


Figure 4. The 2-D cross-section of the vortex tube

the inlet nozzle, whereas the hot flow in the outward region departs the tube across another outlet away from the inlet. The inlet rate of the air is adjusted with flow rates whereas the temperatures of inlet and exit streams are calculated with multiple thermocouples.

Numerical modeling and governing equations

The simulation of the stream field in the vortex tube will be prepared numerically by using FLUENT software package and the flow is considered to be a 3-D compressible, turbulent and steady-state by employing the standard $k-\varepsilon$ turbulence model as it is the best model convergent in turbulence simulation with a good agreement with the experimental results [14]. Finite volume is a numerical technique is applied with 3-D structured mesh for the governing equations of fluid-flow:

– continuity equation:

$$\frac{\partial}{\partial x_j}(\rho u_j) = 0 \quad (1)$$

– momentum equation:

$$\frac{\partial}{\partial x_j}(\rho u_i u_j) = -\frac{\partial p}{\partial x_i} + \left[\mu \left(\frac{\partial u_i}{\partial x_j} + \frac{\partial u_j}{\partial x_i} - \frac{2}{3} \sigma_{ij} \frac{\partial u_k}{\partial x_k} \right) \right] + \frac{\partial}{\partial t}(-\overline{\rho u_i' u_j'}) \quad (2)$$

– energy equation:

$$\frac{\partial}{\partial x_i} \left[u_i \rho \left(h + \frac{1}{2} u_j u_j \right) \right] = \frac{\partial}{\partial x_j} \left[k_{\text{eff}} \frac{\partial T}{\partial x_j} + u_i (\tau_{ij})_{\text{eff}} \right], \quad \text{where } k_{\text{eff}} = k + \frac{c_p \mu_t}{Pr_t} \quad (3)$$

The fluid which considers as working an ideal gas so the state equation is present:

$$p = \rho RT \quad (4)$$

As used the standard $k-\varepsilon$ turbulence model, so turbulence kinetic energy, k , and its rate of dissipation, ε :

$$\frac{\partial}{\partial t}(\rho k) + \frac{\partial}{\partial x_i}(\rho k u_i) = \frac{\partial}{\partial x_i} \left[\left(\mu + \frac{\mu_t}{\sigma_k} \right) \frac{\partial k}{\partial x_j} \right] + G_k + G_b - \rho \varepsilon - Y_M \quad (5)$$

Table 1. Detailed design parameters set-up

Parameters	Value
Length of tube	104 mm
Diameter of tube	8 mm
Diameter of the cold end	5.5 mm
Width of the inlet nozzle	1 mm
Depth of inlet nozzle	1 mm
Number of nozzles	6

$$\frac{\partial}{\partial t}(\rho\varepsilon) + \frac{\partial}{\partial x_i}(\rho\varepsilon u_i) = \frac{\partial}{\partial x_j} \left[\left(\mu + \frac{\mu_t}{\sigma_\varepsilon} \right) \frac{\partial \varepsilon}{\partial x_j} \right] + C_{1\varepsilon} \frac{\varepsilon}{k} (G_k + C_{\varepsilon\varepsilon} G_b) - G_{2\varepsilon} \rho \frac{\varepsilon^2}{k} \quad (6)$$

$$\mu_t = \rho c_\mu \frac{k^2}{\varepsilon} \quad (7)$$

where $C_{1\varepsilon}$ and $C_{2\varepsilon}C_{2\varepsilon}$ are constants. These default amounts have been calculated from experiments with water and air for essential turbulent shear streams containing homogeneous shear streams and weaken isotropic grid turbulence. They have been established to make reasonably well for an enormous domain of wall-bounded and free shear streams. As shown in the equations, several factors and constants have a large influence on the standard k - ε turbulence model [1, 3]. These factors are shown in tab. 2.

Table 2. Definition and values of parameters in the k - ε turbulence model

The factor	Represent	Default value
G_k	Generation of turbulence kinetic energy which caused by mean velocity gradient	-
G_b	Generation of turbulence kinetic energy caused by buoyancy	-
Y_M	Demonstrate the contribution of the fluctuating incompressible turbulence to the overall dissipation rate	-
$C_{1\varepsilon}$	Constant	1.44
$G_{2\varepsilon}$	Constant	1.92
$C_{3\varepsilon}$	Constant	1
c_μ	Constant	0.09
σ_k	The turbulent Prandtl number for k	1.0
σ_ε	The turbulent Prandtl number for ε	1.3

The finite volume method with a 3-D structured mesh is used for solving the governing equations. It can be considered as one of the numerical techniques to characterize intricate stream behavior in the vortex tube. Inlet working fluid (air) is assumed as a compressible, it means that (specific heat, thermal conductivity, and dynamic viscosity) are put to be constant over the procedure of the numerical analysis. To discretize convective terms, the second-order upwind scheme is employed, whereas and SIMPLE algorithms are utilized to solve the momentum and energy equations simultaneously. Due to considerable non-linear and coupling effects of the governing equations, lower under-relaxation factors varied from 0.1 to their default value are put for the pressure, density, body forces, momentum, k , ε , turbulent viscosity, and energy components to ensure the stability and convergence of the iterative calculations.

An important parameter in the vortex tube study is α which is defined as a cold mass fraction:

$$\alpha = \frac{\dot{m}_c}{\dot{m}_{in}} \quad (8)$$

The cold and hot exit temperature differences (ΔT_c and ΔT_h , respectively) are defined:

$$\Delta T_c = T_i - T_c \quad \text{and} \quad \Delta T_h = T_h - T_i \quad (9)$$

Vortex tube physical modeling and boundary condition

The CFD models are considered based on this new experimental analysis 3-D with a standard $k-\varepsilon$ turbulence model. As inlet air is assumed to be a working fluid and as a compressible so the other parameters will be assumed as constant values (dynamic viscosity, specific heat, and thermal conductivity) during this analysis. To solve the momentum and energy equations, SIMPLE algorithm will be used and due to non-linear and coupling virtue is very high of the governing equations, for the density, pressure, momentum, energy, body forces, k , ε , and turbulent viscosity components, lower under-relaxation factors will take varied from 0.1 to their default value to make sure the stability and convergence of the iterative calculations. In order to reduce the computations, models are considered to be rotational periodic and only 1/6 sector of the stream domain CFD model will be considered, as demonstrates the 3-D model in figs. 5(a) and 5(b). At inlets of the nozzle, the air is compressed into the tube with inlet gas temperature (stagnation temperature) is fixed at 293 K, pressure inlet is varied from 4 bar to 6 bar, and the cold mass fraction 0.3 to 0.8. The pressure will be adjusted to vary with the cold mass fraction ant the hot outlet. The no-slip velocity boundary condition is enforced on all of the walls of the vortex tube, and it is assumed to be adiabatic.

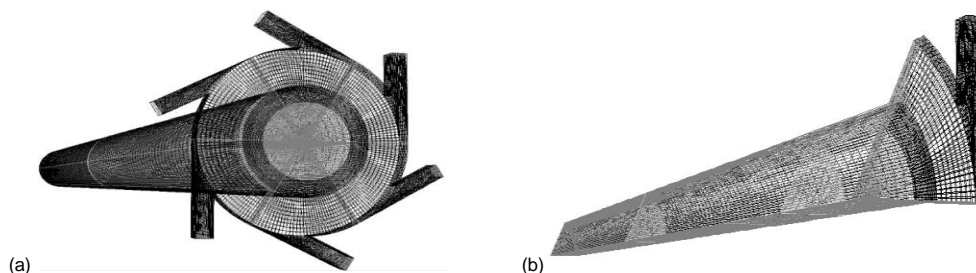


Figure 5. (a) The 3-D CFD model of vortex tube, (b) a sector of the CFD model

The CFD results and experimental data comparisons

Due to the importance of temperature separation in the vortex tube device; most researches choose this parameter for validation of their CFD results [19]. As shown below, the figs. 6 and 7 show the comparisons between the CFD simulation and the experimental data, It can be noticed a good agreement between the results. As the results show, when the cold mass fraction increase, the ΔT_c increases, and a maximum value occurs at $\alpha = 0.3$. The comparisons of the CFD simulation and the experimental results are shown in parameters of the inlet pressure and mass-flow rate has a well predict with a deviation of calculated data is less than or equal to 7.79% for the cold temperature difference, as shown in figs. 6 and 7.

Experimental results

An approximation study was executed by Stephan *et al.* [20] for geometrical parameters like straight nozzles vortex tubes and statement as the ratio of the actual temperature drop of the cold air that departure from exhaust to the maximum temperature difference ($\Delta T_c / \Delta T_{c,max}$) may be specified as of cold mass fraction function:

$$\frac{\Delta T_c}{\Delta T_{c,max}} = f(\alpha) \quad (11)$$

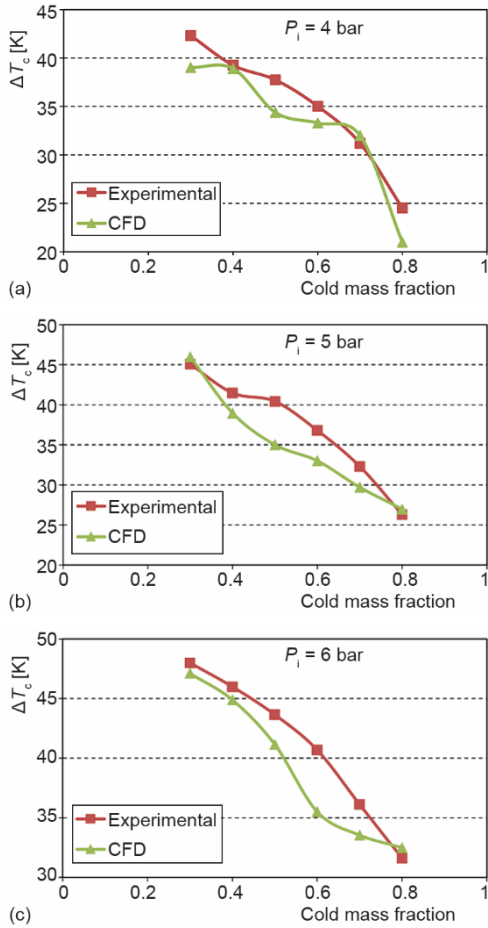


Figure 6. Comparison of different inlet pressure in terms of cold exit temperature difference

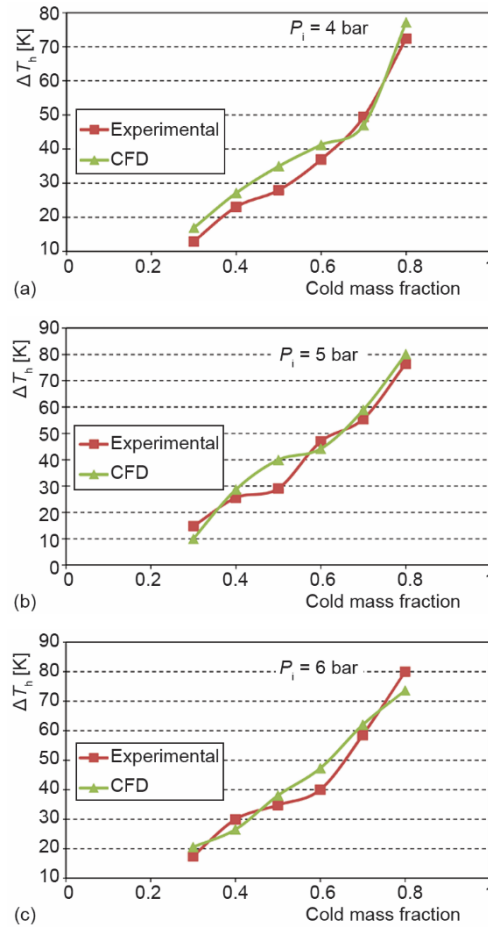


Figure 7. Comparison of different inlet pressure in the terms of hot exit temperature difference

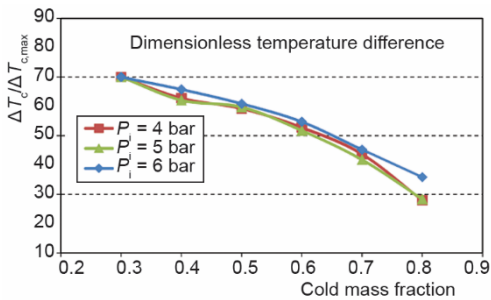


Figure 8. Non-dimensional cold temperature difference vs. cold mass fraction

For the vortex tube the ratio of $\Delta T_c/\Delta T_{c,max}$ is not dependent on the inlet pressures and may be determined as a function of the cold mass fraction. The similitude relation $\Delta T_c/\Delta T_{c,max}$ as a function of α may be gotten and indicated in fig. 8. It expressed:

$$\frac{\Delta T_c}{\Delta T_{c,max}} = 20.412\alpha^4 - 48.032\alpha^3 + 39.788\alpha^2 - 14.396\alpha + 2.8687 \quad (12)$$

Numerical results

To eliminate and reduce any errors due to the coarseness or inappropriate dimensions of the fluid field mesh and the independence of the analysis results from the effects of meshing, numerical modeling was conducted with different mesh sizes to investigate the effect of the number of meshes [21]. For this purpose, eight models are made in the number of different elements and the results are based on the important parameter of the temperature difference and are shown in fig. 9. The results indicate that for a total number of more than 151000 elements, the change in results is negligible. As a result, due to the stability of the results and the independence of the numerical results from the grid effects, the same number of elements is used to reduce the computational time for all models. The temperature contours in the longitudinal section for the chosen models show in fig. 10. The circumstance stream is hot, and the center stream is cold and showing an increase of temperature radial direction.

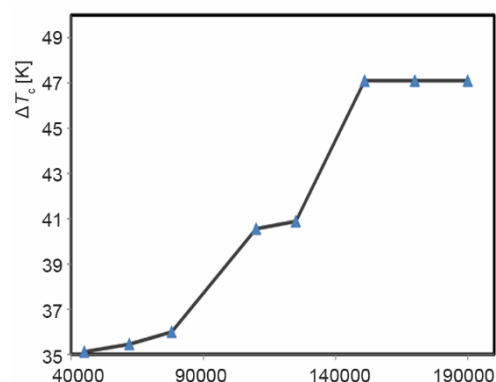


Figure 9. Grid independent study based on hot exit temperature difference, ΔT_c

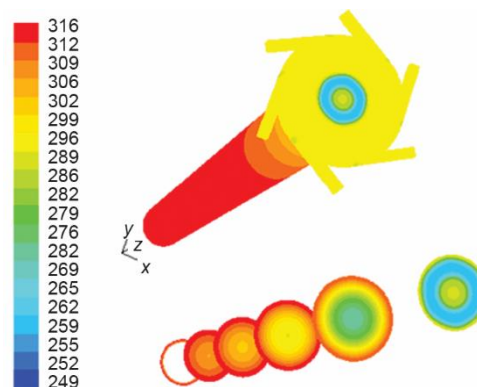


Figure 10. Temperature distribution in longitudinal section for $P_i = 6$ bar and $\alpha = 0.3$

The maximum total pressure appears to close the peripheral of the tube surface in all CFD models simulations of the vortex tubes. The total pressure profiles appear as a rise in the pressure amounts towards the peripheral. Both total and static pressures rise with rising the inlet pressures and α as present in figs. 11 and 12.

Figures 13, and 14 show ($Z/L = 0.2, 0.5,$ and 0.8) for the cold mass fraction of 0.3-0.8 present a comparing of the velocity components, it is clear that swirl velocity has the largest amount. The radial profile of the swirl velocity suggested a free vortex nearby the surface and the amounts can be assumed very small at the center. Figure 13 indicates that the higher the inlet pressure the higher the swirl. Increasing the distance from the inlet zone towards the hot end the swirl velocity magnitude decreases in all models. The fluid at the core of the vortex tube has deficient kinetic energy because the swirl velocity at the center region is minimum. The radial profiles for the axial velocity at $Z/L = 0.2, 0.5,$ and 0.8 are presented in fig. 14.

For the $P_i = 5$ bar at the axial position of $Z/L = 0.2, 0.5,$ and 0.8 the axial velocity was maximum at 93, 67, and 61 m/s, respectively. Therefore, a maximum amount of 93 m/s is view at the tube axis nearby the inlet region ($Z/L = 0.2$).

Power separation analysis

The performance features of the vortex tubes have been estimated by the COP. As shown in figs. 15 and 16, COP_{he} decreases and COP_{re} increases with increasing α for different inlet pressures. It may be noticed that the COP of the vortex tube varies from 0.25 to 0.74.

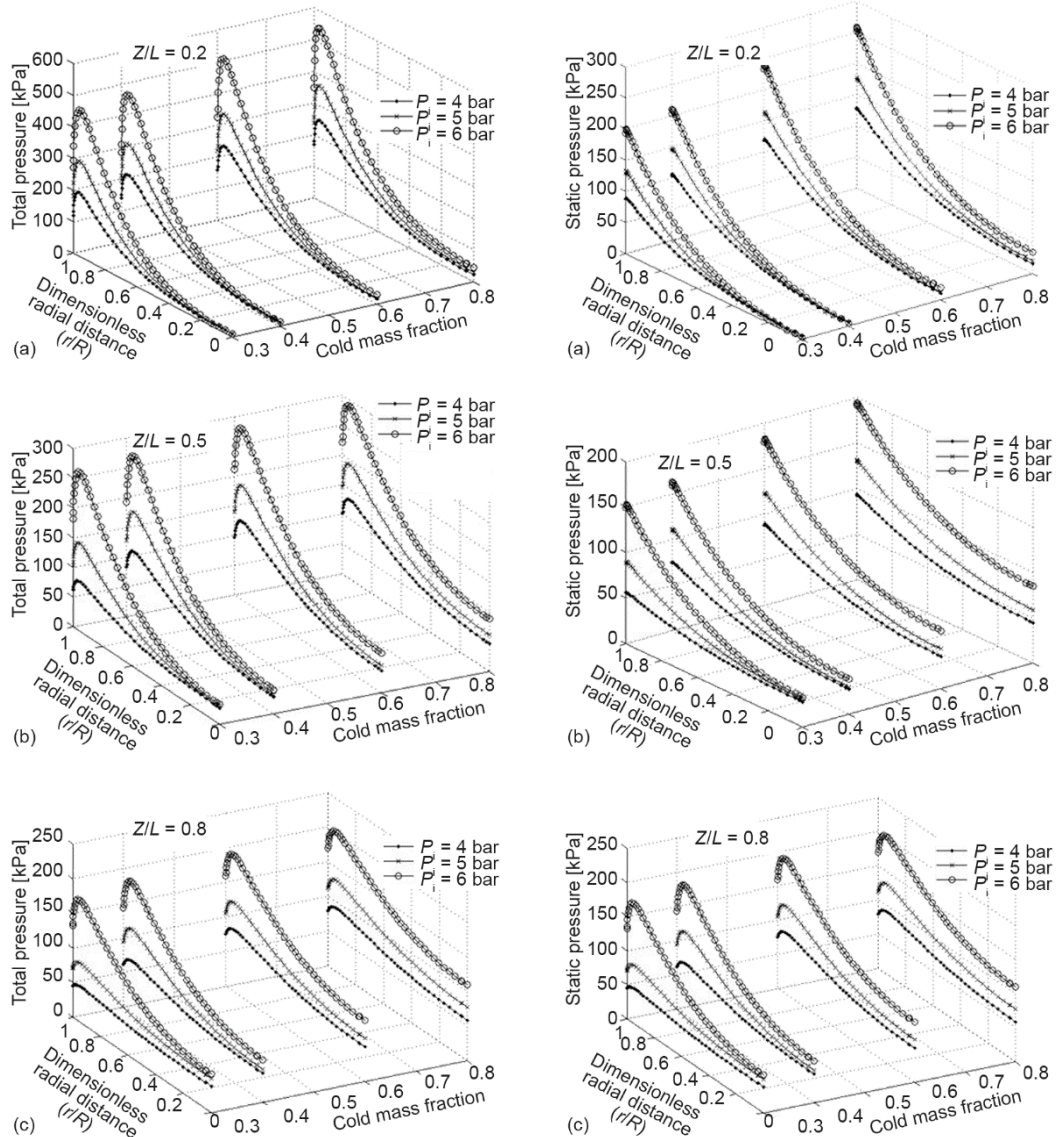


Figure 11. Radial profiles of total pressure at different axial locations

Figure 12. Radial profiles of static pressure at different axial locations

Conclusion

Although even through years, various investigations for the separation of the energy in the vortex tube have been presented but unfortunately without a well-accepted explanation

for the physical process because the internal flow complexity so that the aims of this study will be focused on the flow characteristics inside the vortex tube and optimizing vortex tube performance with new experimental model investigation and CFD analysis. The experiment model

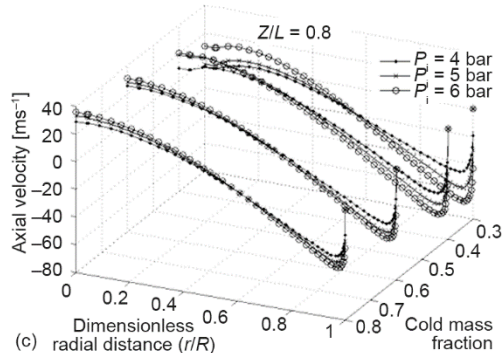
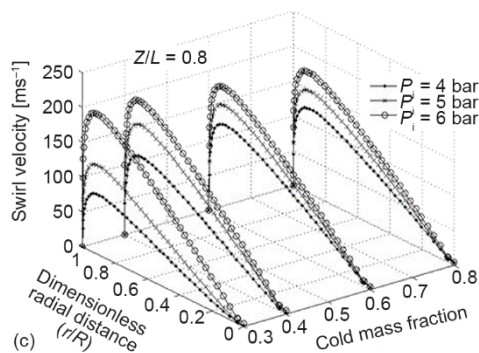
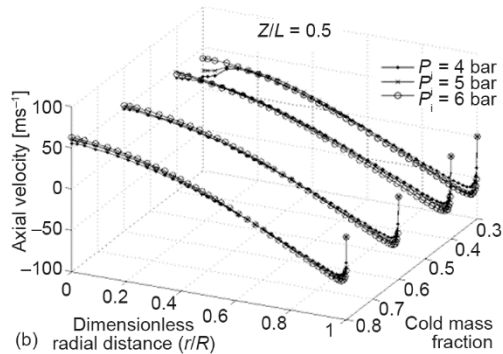
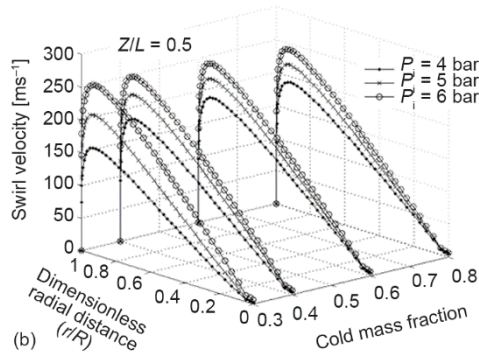
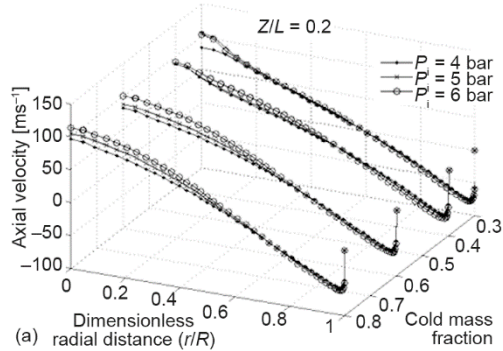
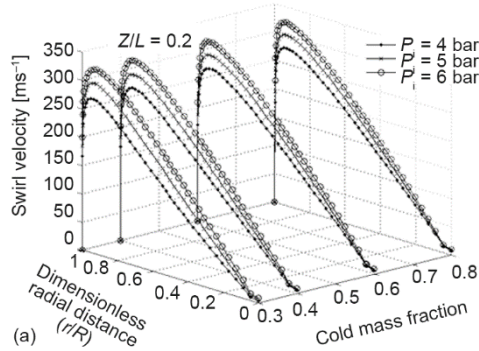


Figure 13. Radial profiles of swirl velocity at different axial locations

Figure 14. Radial profiles of axial velocity at different axial locations

was performed in the vortex tube with a total length of 104 mm and an inner diameter of 8 mm, made of cast iron. Three different inlet pressures (6, 5, and 4 bar) with stagnation temperature 293 K were tested. The results of the experimental investigation of the vortex tube are for the cold and hot air outlet temperatures with the dimensionless cold mass fraction (0.3-0.8) and the air pressures as inlet parameters. The experiment model was tested and investigated with three-dimensional CFD with a standard $k-\epsilon$ turbulence model using FLUENT software package to

investigate the energy separation and the velocity distributions. The comparisons between the experimental investigation and the CFD model have a good agreement with a deviation of less than or equal to 7.79%. As increasing of the cold mass fraction, the ΔT_c increases and a

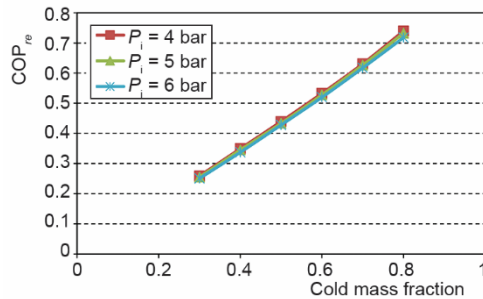


Figure 15. The COP_{re} at different nozzles

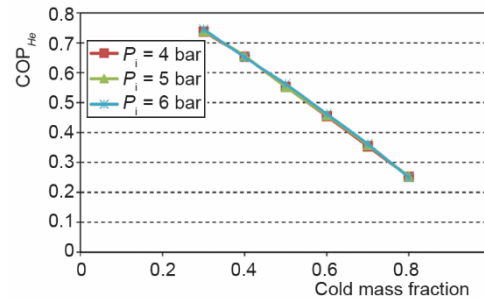


Figure 16. The COP_{he} at different nozzles

maximum value occurs at $\alpha = 0.3$, as well as increasing of the inlet pressure causes increasing ΔT_c , where the maximum value occurs at $P = 6$ bar (ΔT_c experimental = 48.34 K and ΔT_c numerical = 47.1 K). In all simulated CFD models for the vortex tube, the maximum total pressure happened nearby the peripheral of the tube wall which an increase of the pressure values profiles shows towards the periphery. A various axial location ($Z/L = 0.2, 0.5,$ and 0.8) and cold mass fraction of $0.3-0.8$ was modeled in order to evaluate swirl velocity and radial profiles with respect to different inlet pressures. The maximum axial velocity occurs at the tube axis nearby the inlet exit ($Z/L = 0.2$) was found 93. The COP of the vortex tube ranged from 0.25 to 0.74.

Nomenclature

H	– height of nozzle, [mm]
L	– length of vortex tube, [mm]
P	– pressure, [Pa]
T	– temperature, [K]
Z	– axial direction along the tube
ΔT_c	– temperature difference between inlet and cold end, [K]
ΔT_h	– temperature difference between hot end and inlet, [K]

<i>Greek symbol</i>	
α	– cold gas fraction
<i>Subscripts</i>	
c	– cold
h	– hot
i	– inlet

References

- [1] Pourmahmoud, N., *et al.*, Computational Fluid Dynamics Analysis of the Influence of Injection Nozzle Lateral Outflow on the Performance of Ranque-Hilsch Vortex Tube, *Thermal Science*, 18 (2014), 4, pp. 1191-1201
- [2] Ranque, G. J., Experiments on Expansion in a Vortex with Simultaneous Exhaust of Hot Air and Cold Air, *Le J. De Phys.*, 4 (1933), pp. 1125-1130
- [3] Pourmahmoud, N., *et al.*, Numerical Simulation of Secondary Vortex Chamber Effect on the Cooling Capacity Enhancement of Vortex Tube, *Heat Mass Transf.*, 50 (2014), 9, pp. 1225-1236
- [4] Hilsch, R., The Use of Expansion of Gases in a Centrifugal Field as a Cooling Process, *Rev. Sci. Inst.*, 13 (1947), 2, pp. 108-113
- [5] We, Y., *et al.*, Modification and Experimental Research on Vortex Tube, *Int. J. Refrig.*, 30 (2007), 6, pp. 1042-1049
- [6] Ahlborn, B., Groves, S., Secondary Flow in a Vortex Tube, *Fluid Dyn. Res.*, 21 (1997), 2, pp. 73-86
- [7] Promvongse, P., Eiamsa-ard, S., Investigation on the Vortex Thermal Separation in Vortex Tube Refrigerator, *Sci. Asia*, 31 (2005), 3, pp. 215-223

- [8] Aydin, O., Baki, M., An Experimental Study on the Design Parameters of a Counter Flow Vortex Tube, *Energy*, 31 (2006), 14, pp. 2763-2772
- [9] Markal, B., *et al.*, An Experimental Study on the Effect of the Valve Angle of Counter-Flow Ranque-Hilsch Vortex Tubes on Thermal Energy Separation, *Exp. Therm. Fluid Sci.*, 34 (2010), 7, pp. 966-971
- [10] Xue, Y., *et al.*, Experimental Study of the Flow Structure in a Counter Flow Ranque-Hilsch Vortex Tube, *Int. J. Heat Mass Transfer*, 55 (2010), 21-22, pp. 5853-5860 .
- [11] Aljuwayhel, N. F., *et al.*, Parametric and Internal Study of the Vortex Tube Using a CFD Model, *Int. J. Refrigeration*, 28 (2005), 3, pp. 442-450
- [12] Eiamsa-ard, S., Promvongse, P., Numerical Investigation of the Thermal Separation in a Ranque-Hilsch Vortex Tube , *Int. J. Heat Mass Trans.*, 50 (2007), 5-6, pp. 821-832
- [13] Farouk, T., Farouk, B., Large Eddy Simulations of the Flow Field and Temperature Separation in the Ranque-Hilsch Vortex Tube, *Int. J. Heat Mass Trans.*, 50 (2007), 23-24, pp. 4724-4735
- [14] Pourmahmoud, N., *et al.*, Numerical Investigation of Operating Pressure Effects on the Performance of a Vortex Tube, *Thermal Science*, 18 (2014), 2, pp. 507-520
- [15] Kandil, H. A., Abdelghany, S. T., Computational Investigation of Different Effects on the Performance of the Ranque-Hilsch Vortex Tube, *Energy*, 84 (2015), May, pp. 207-218
- [16] Niknam, H., *et al.*, Numerical Investigation of a Ranque-Hilsch Vortex Tube Using a 3-Equation Turbulence Model, *Chemical Eng. Com.*, 204 (2017), 3, pp. 327-336
- [17] Hassanzadeh, A., *et al.*, Numerical Simulation of Motion and Deformation of Healthy and Sick Red Blood Cell through a Constricted Vessel Using Hybrid Lattice Boltzmann-Immersed Boundary Method, *Computer Methods in Biomech. Biomed. Eng.*, 20 (2017), 7, pp. 737-749
- [18] Dawoodian, M., *et al.*, CFD and Experimental Analysis of Drag Coefficient and Flow Field's Manner in a Parachute for Various Reynolds Numbers and Different Vent Ratios, *ISRN Aerospace Eng.*, V. 2013 (2013), ID 320563
- [19] Behera, U., *et al.*, CFD Analysis and Experimental Investigations towards Optimizing the Parameters of Ranque-Hilsch Vortex Tube, *Int. J. Heat Mass Transfer*, 48 (2005), 10, pp. 1961-1973
- [20] Stephan, K., *et al.*, An Investigation of Energy Separation in a Vortex Tube, *Int. J. Heat Mass Transfer*, 26 (1983), 3, pp. 341-348
- [21] Babil, A. K., Razavi, S. E., On the Thermo Flow Behavior in a Rectangular Channel with Skewed Circular Ribs, *Mech. & Ind.*, 18 (2017), 2, ID 225